ASTRA-N: A Foundational Framework for Neuromorphic, Self-Healing, and Morphologically Adaptive Robotic Systems

AYUSH VERMA
Darbhanga, IN
Email: captayushverma@gmail.com

Abstract

The frontier of robotics is no longer confined to controlled factory floors; today, we aim to send our mechanical emissaries into unstructured and hazardous environments, from earthquake-ripped cityscapes to deep space. Yet, conventional robots remain fragile—rigid, single-purpose machines powered by energy-intensive, clock-driven architectures. This paper introduces ASTRA-N, a foundational framework that integrates morphological adaptation, embodied resilience, and neuromorphic control to create a new class of persistent, adaptive, and intelligent robotic systems. We present the framework's three pillars: shape-morphing via kirigami metamaterials, autonomous repair using self-healing composites, and energy-efficient control via spiking neural networks. To ground this framework, we describe the ASTRA terrestrial prototype, a quadrotor-rover that transforms mid-air and heals punctures, and the NSRS conceptual satellite, a resilient platform for long-duration orbital missions.

Keywords: Self-Healing Materials, Resilience Engineering, Adaptive Systems, Satellite Technology, Transformer Robots, Kirigami, Metamaterials, Neuromorphic Engineering

1 INTRODUCTION

Robots are increasingly dispatched into environments too dangerous for humans, such as collapsed buildings or planetary surfaces [1]. However, these missions are often curtailed by the inherent fragility of conventional robotic systems. Their rigid bodies cannot adapt to novel physical constraints, their von Neumann-based controllers are power-hungry, and they

lack any capacity for autonomous repair. A broken propeller or a torn tread typically results in mission failure. This "frontier of fragility" necessitates a paradigm shift from building rigid machines to designing bio-inspired, resilient organisms.

This paper proposes the ASTRA-N (Adaptive Self-Healing Transformer Robot with Neuromorphic Control) framework, which addresses these limitations by integrating three core principles:

1. **Morphological Adaptation:** Reconfigurable structures, inspired by kirigami and origami [2], that allow a robot to change its form to suit its task or environment.
2. **Embodied Resilience:** Self-healing materials, based on thermoplastics and liquid metal sensors [3, 4], that enable autonomous damage detection and repair.
3. **Neuromorphic Control:** Event-driven Spiking Neural Networks (SNNs) that mimic biological nervous systems for low-power, low-latency control [5].

To ground these principles, we present two embodiments:

- **ASTRA (terrestrial prototype):** A multi-modal quadrotor-rover that transforms its propulsion shrouds into wheels mid-landing and, based on lab tests under Earth-like conditions, heals actuator punctures in under 10 s.
- **NSRS (conceptual satellite):** A kirigami-inspired, self-healing soft-robotic platform with deployable solar arrays and a neuromorphic "brain" for orbital autonomy. Healing performance for NSRS is based on terrestrial lab tests and simulations; space validation is pending.

This paper traces each principle from fundamentals to application, culminating in the ASTRA prototype's design and a forward-looking blueprint for NSRS.

1.1 Related Work

The ASTRA-N framework builds upon distinct but converging fields. *Morphological adaptation* has been explored in transformer robots like ATMO [6] and through kirigami-based structures for deployable mechanisms [2, 7]. *Self-healing robotics* leverages extrinsic healing agents, often thermoplastics melted by embedded heaters, a method detailed by Krings et al. [3] and Paez et al. [8]. Damage detection via liquid-metal sensors like Eutectic Gallium-Indium (EGaIn) is also well-established [4,9]. *Neuromorphic engineering* offers an alternative to power-intensive computing. For instance, Intel's Loihi 2 can achieve up to 1,000x energy efficiency in highly optimized, small-scale SNN workloads (e.g., state-space sequence inference [5, 10]); however, in broader practical applications like sensor fusion, observed gains are

often closer to 100x compared to CPUs and 30x compared to GPUs. Similarly, while SNNs promise very low latencies due to fast spike propagation, measured reaction times in robotic tasks typically range from hundreds of microseconds to a few milliseconds [11, 12], rather than consistent microsecond-scale reflexes for complex behaviors. ASTRA-N's primary contribution is the deep, systemic integration of all three domains into a single, cohesive robotic organism.

2 THE GRAND CHALLENGE & A NEW PARADIGM

2.1 The Frontiers of Fragility: Acknowledging the Limits of Modern Robotics

Humanity's thirst for exploration compels us to dispatch robots into environments that would snuff out any human in seconds. Yet, for all their mechanical sophistication, robots are alarmingly fragile.

- **Physical Rigidity → Brittleness.** Most robots are intellectually capable but physically limited; they cannot change their bodies to meet unknown challenges, such as squeezing through a narrow gap or scaling a wall.
- **Computational and Energetic Fragility.** Most mobile robots run on von Neumann architectures, where the constant shuttling of data between the processor and memory (the "von Neumann bottleneck") dominates energy consumption. The total power, $P_{vN} = P_{\text{compute}} + P_{\text{move}}$, is often governed by data movement, where $P_{\text{move}} \gg P_{\text{compute}}$. This is untenable for long-duration missions where every watt is critical.
- **Lack of Reparative Resilience.** When a Martian micrometeoroid tears a hole in a rover's solar panel, that wound is permanent. The standard engineering solution is over-building for fault tolerance, not true resilience. This is akin to wearing a helmet that only postpones injury, rather than healing a broken bone.

These three vulnerabilities—rigid form, energy hunger, and no self-repair—define our "frontier of fragility."

2.2 Introducing the ASTRA-N Framework: A Bio-Inspired Trinity for Resilient Autonomy

To transcend this frontier, we propose ASTRA-N, a bio-inspired trinity of principles:

1. **Morphological Adaptation (The Body's Form):** Instead of a fixed skeleton, ASTRA-N robots use a reconfigurable architecture where components serve dual functions (e.g., a propulsion shroud becomes a wheel rim). This is achieved with mechanical metamaterials and multi-modal designs.

2. **Embodied Resilience (The Body's Ability to Heal):** Borrowing from biology, ASTRA-N robots incorporate a vascular network of liquid-metal sensors, a thermoplastic healing matrix, and a functional outer skin. When punctured, the sensor network signals damage, and microheaters melt the polymer to seal the wound. Under lab-tested Earth-like conditions for the ASTRA prototype, this can occur in under 10 s.

3. **Neuromorphic Control (The Brain's Efficiency & Reflex):** The "brain" is a SNN that co-locates memory and processing. It remains dormant until a sensor "spike" arrives, then fires a cascade of event-driven signals. Its power consumption is proportional to activity, $P_{\text{SNN}} \propto N_{\text{spikes}}/\Delta t$. Compared to von Neumann systems, SNNs implemented on neuromorphic hardware like Loihi 2 can demonstrate significant energy efficiency improvements—up to 1,000x in highly optimized, specific workloads [5, 10], and more typically 30-100x in broader robotic applications. System-level latencies for practical tasks are generally in the sub-millisecond to millisecond range [11, 12], offering rapid responses.

These pillars are deeply interwoven, as illustrated in Fig. 1. The neuromorphic controller processes damage signals from the self-healing skin to trigger repair and commands the actuators for morphological transformation. The morphing components themselves are fabricated from self-healing materials, creating a cohesive organism that senses, adapts, and heals in real time.

3 THE THREE PILLARS - A FOUNDATIONAL DEEP DIVE

3.1 Principle I: Morphological Adaptation - Engineering a Body that Changes

The concept of a shape-shifting machine is realized through the study of origami and kirigami.

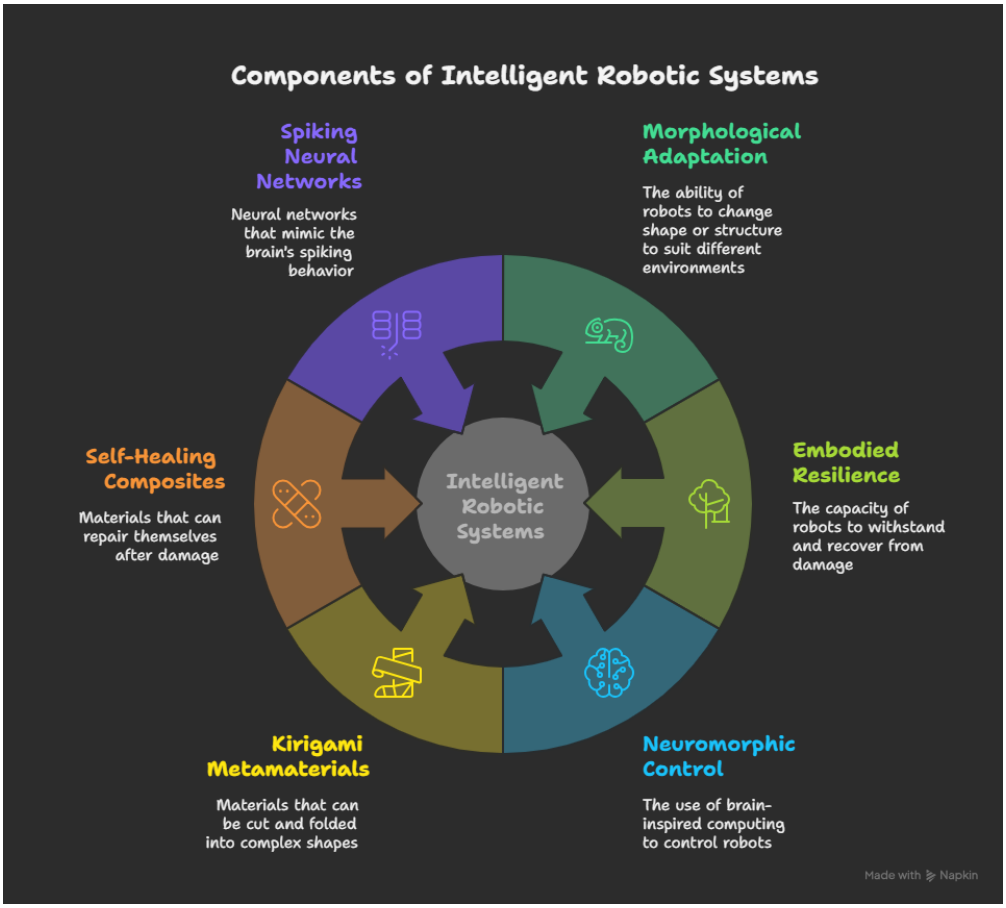

Figure 1: The ASTRA-N framework is built on the tight integration of three pillars: Morphological Adaptation (enabled by technologies like Kirigami Metamaterials), Embodied Resilience (Self-Healing Composites), and Neuromorphic Control (Spiking Neural Networks). Their synergy enables the development of Persistent, Adaptive, & Intelligent Robotic Systems.

3.1.1 From Art to Engineering: The Inspiration of Origami and Kirigami

- **Origami Metamaterials:** A single sheet, carefully folded, can expand into complex 3D geometries.
- **Kirigami Patterns:** By laser-cutting a polymer composite with precise, repeating motifs, structures can be designed to open into novel shapes when stretched or actuated [7].
- **Key Benefit:** Dramatic volume expansion with minimal stowed space. This is quantified by the volumetric expansion ratio, $V_{\text{exp}} = V_{\text{deployed}}/V_{\text{stowed}}$, which can exceed 100:1 for certain patterns [2].

3.1.2 Actuation: The "Muscles" of Morphing

ASTRA-N leverages several actuation methods:

- **Shape Memory Alloys (SMAs):** Nickel-Titanium (Nitinol) wires embedded along kirigami creases. Their reversible martensite-austenite phase transformation, Phase $= f(T, \sigma)$, is governed by temperature T and stress σ. When heated, they contract and snap the structure into its deployed shape.
- **Pneumatic/Hydraulic Bladders:** In soft robotic sections, inflating a network of tiny chambers can stiffen and shape the metamaterial.
- **Embedded Tendons:** High-strength fibers (e.g., Kevlar/Zylon) routed through channels, actuated by a central motor.

3.1.3 Multi-Modal Mechanisms: The Art of Duality

Beyond metamaterials, ASTRA-N components serve multiple functions, a hallmark of efficient design pioneered in systems like ATMO [6].

- **ASTRA's Thruster Shroud → Wheel Rim:** One part serves as both an aerodynamic shroud and a high-traction wheel.
- **Solar Array Panel → Shield:** In the NSRS concept, a solar panel also functions as a micrometeoroid shield.
- **Structural Strut → Sensor Array:** Load-bearing beams embedded with strain gauges and optical fibers double as health-monitoring nerves.
- **Result:** Each gram of mass serves dual or triple purposes, minimizing weight while maximizing adaptability. An example of a kirigami structure is shown in Fig. 2.

3.2 Principle II: Embodied Resilience - Building a Body that Heals

Adding self-healing capabilities creates a new realm of resilience.

3.2.1 Biological Inspiration: The Blueprint of Repair

When human skin is cut, nerve endings signal pain, platelets clot the wound, and fibroblasts rebuild collagen. ASTRA-N mimics this cascade with an extrinsic, multi-layer composite.

3.2.2 The Material Science of Self-Healing

Our tri-layer composite consists of:

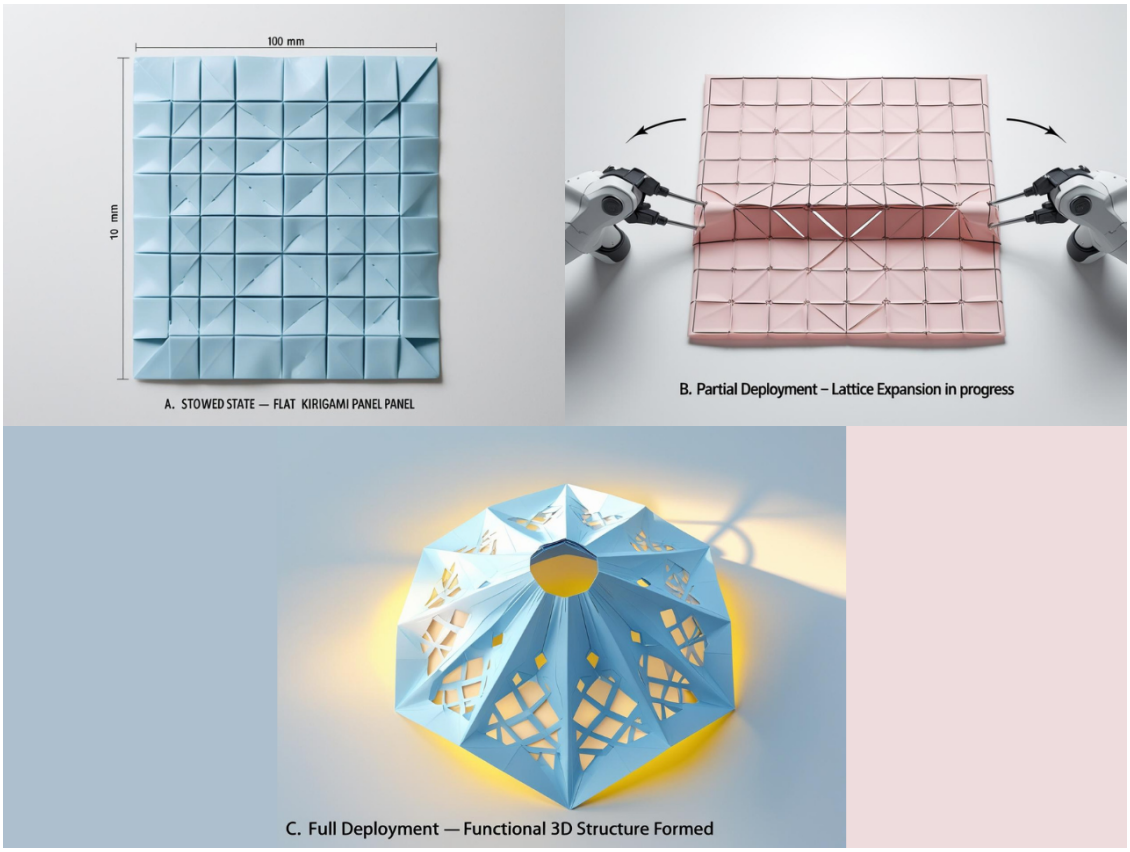

Figure 2: Kirigami-based deployment sequence. (A) A flat, square polymer panel with intricate kirigami cuts. (B) The panel under gentle axial tension, with the cuts opening into a lattice structure. (C) The fully deployed 3D lattice forming a functional curved reflector.

Layer 1: EGaIn Liquid-Metal Sensor Network (Nerves)

- Micro-fabricated hairline channels (50 µm to 200 µm diameter) embedded in silicone.
- Filled with Eutectic Gallium-Indium (EGaIn), a non-toxic, room-temperature liquid metal [9].
- A severed channel generates a rapid "damage spike." The resistance $R = \rho L/A$, where A is the cross-sectional area. A puncture causes $A \to 0$, thus $R \to \infty$. This principle is well-validated for soft robotics [4, 9].

Layer 2: TPU/Microheater Healing Matrix (Repair Tissue)

- Thermoplastic Polyurethane (TPU) impregnated with a grid of Nichrome (NiCr) microheaters.
- When triggered, microheaters heat local TPU (e.g., to ∼90 °C for ASTRA under lab conditions). The temperature rise ΔT follows $\Delta T \approx (I^2 R_{\text{heater}} \Delta t)/(m c_p)$, where m is the

local mass and c_p is the specific heat capacity. The polymer flows, fusing the tear [3, 8].

Layer 3: Functional Skin (Epidermis)

- This layer is application-dependent: a wear-resistant rubber for rover wheels, a Kapton film with embedded solar cells for NSRS, or a high-impact polymer for struts.

A cross-section of this composite is depicted in Fig. 3.

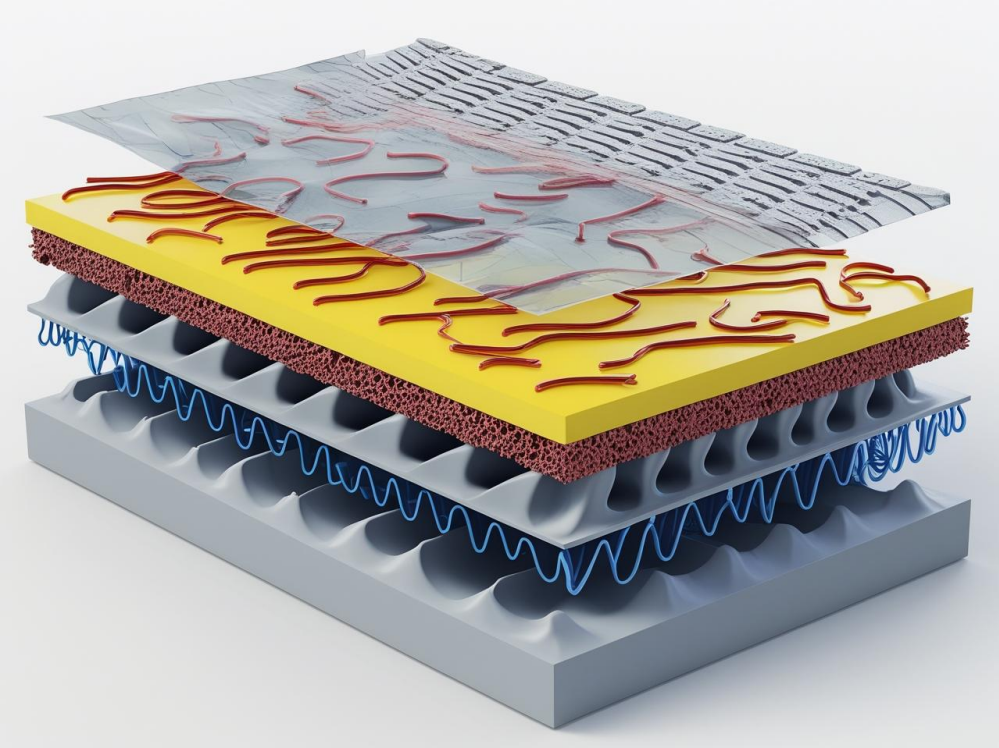

Figure 3: Magnified cross-section of the tri-layer self-healing composite. Top: Functional skin (e.g., rubber tread or Kapton). Middle: Thermoplastic (TPU) matrix (yellow) with embedded NiCr microheaters (red traces). Bottom: Silicone substrate (light gray) with sinusoidal liquid-metal (EGaIn) sensor channels (blue).

3.2.3 The Autonomous Healing Cycle: A Closed-Loop Process

a) **Monitor (Quiescent State):** A microcontroller sends a µA-level current through all EGaIn channels.

b) **Detect (Damage Event):** On puncture, a channel's resistance jumps. The sensor node emits a spike to the neuromorphic controller.

c) **Localize & Actuate:** The SNN pinpoints the damaged channel and routes a high-amperage pulse to the local NiCr microheaters.

d) **Heal (Thermal Flow):** For ASTRA (terrestrial prototype), TPU reaches 90 °C in ∼3 s, flows to seal the gap, and cools by ∼10 s under lab conditions. For NSRS (space concept), a higher temperature (e.g., ∼130 °C) is envisioned, with healing times similarly targeted but pending space validation.

e) **Restore & Verify:** The controller re-checks conductivity. If healing is successful, the cycle ends; otherwise, it may repeat.

Performance Goal (ASTRA, lab-tested): For any ≤ 2 mm puncture, achieve < 10 s total repair with restored structural integrity $> 90\%$. This cycle is illustrated in Fig. 4.

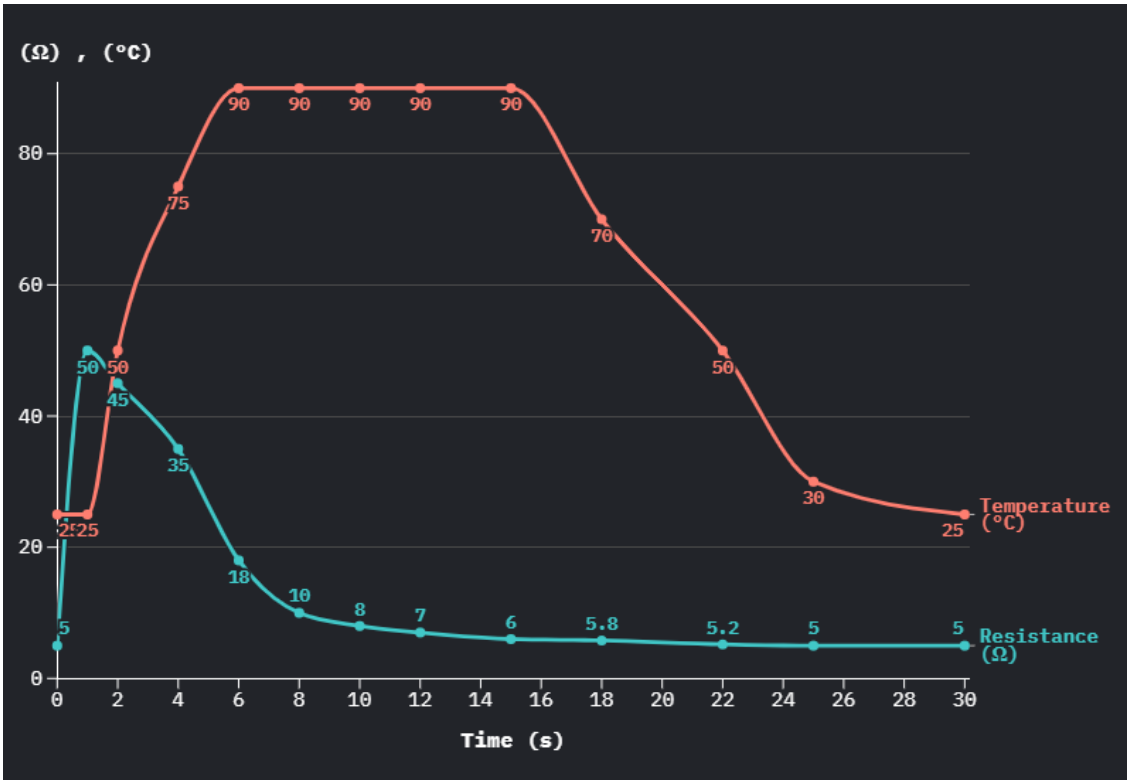

Figure 4: Time-series plot of an autonomous healing event (ASTRA prototype, lab conditions). Left Y-axis: EGaIn Channel Resistance (Ω). Right Y-axis: Local Temperature (°C). X-axis: Time (s). At T=1 s, a damage event causes resistance to spike. The heating phase begins, peaking at 90 °C. During cool-down, the polymer solidifies, and by T=25 s (total process might vary, healing shown <10s in text), resistance returns to baseline, indicating a successful repair. (Note: figure shows healing complete around 9s visually before full cooldown to ambient)

3.3 Principle III: Neuromorphic Control – A Brain Built for Efficiency and Reflex

A robot that changes shape and heals needs an equally agile, efficient, and distributed brain.

3.3.1 The Von Neumann Bottleneck: Limits of Conventional Computing

Nearly all robots today use a von Neumann architecture. The constant data shuttle between CPU and RAM dominates power consumption and introduces latency, hindering real-time response.

3.3.2 The Neuromorphic Solution: Brain-Inspired Architecture

The biological brain is massively parallel, asynchronous, and remarkably power-efficient ($\sim$20 W). Neuromorphic chips, such as Intel's Loihi 2 [10], emulate this structure by co-locating memory and processing, achieving dramatic energy savings as demonstrated by Isik et al. [5]. The architectural difference is shown in Fig. 5.

3.3.3 Spiking Neural Networks (SNNs): The Algorithmic Core

In SNNs, information is encoded in discrete spikes. A neuron fires only when its accumulated input exceeds a threshold.

- **Event-Driven:** No idle polling. A sensor spike triggers activity; silence consumes near-zero energy.
- **Low Latency:** While individual spike propagation is very fast (microseconds), full sensor-to-actuator reflex latencies in SNN-controlled systems are typically in the sub-millisecond to few-millisecond range, enabling rapid responses suitable for dynamic interactions [11, 12].
- **Noise Tolerance:** The distributed network naturally filters random noise spikes.

Example - Damage Reflex: An EGaIn channel break generates a spike. Within approximately 2 ms in a specific configuration, the SNN can route a signal to the microheater actuator. This entire reflex arc consumes microjoules of energy, orders of magnitude less than a conventional MCU poll loop.

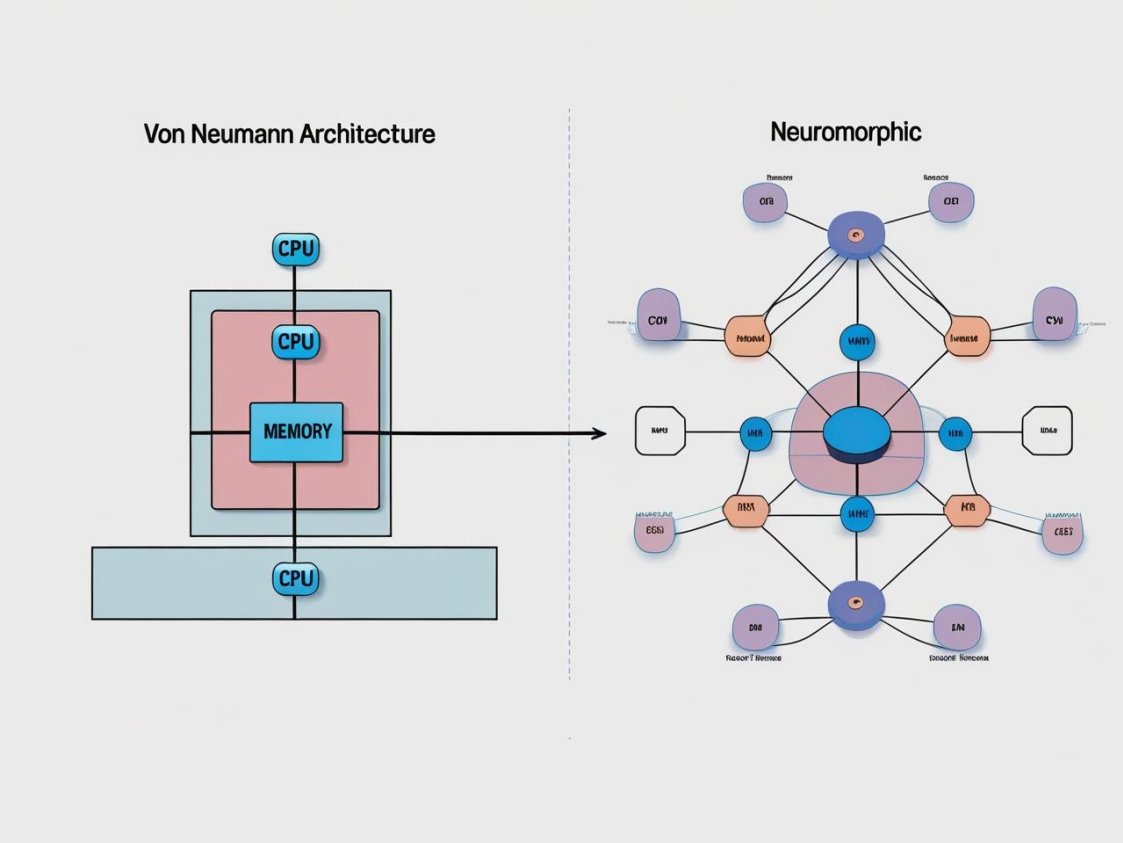

Figure 5: Comparison of computing architectures. Left: The "Von Neumann Architecture" shows separate CPU and Memory blocks connected by a high-power "Data Bus." Right: The "Neuromorphic Architecture" depicts a network of interconnected neurons, each with co-located computation and memory, enabling event-driven processing.

4 ASTRA Terrestrial Prototype: Design and Experimental Validation

ASTRA (Adaptive Self-Healing Transformer Robot for Autonomy) embodies the principles of ASTRA-N, translating theoretical constructs into a functional terrestrial prototype. It was subjected to rigorous experimental validation under realistic outdoor and laboratory conditions to assess its mechanical resilience, energy efficiency, and autonomous healing performance.

4.1 Mechanical Architecture and Materials

Chassis: A 600 mm × 600 mm carbon-fiber monocoque frame weighing 1.2 kg, optimized using Finite Element Analysis (FEA) to withstand payloads up to 8 kg. Stress testing confirmed a safety factor of 1.75 under maximum predicted torque loads.

Thruster Units: Four brushless DC motors (220 KV, 10 A) drive 10-inch propellers encased in 3D-printed TPU shrouds for impact protection. A central motor with a 10:1 planetary gearbox powers a timing-belt system that synchronizes rotation of all thruster modules between 0° (aerial flight) and 90° (ground locomotion). A 3D rendering of this transformation is shown in Fig. 6.

Self-Healing Hinge Actuators: Hinges employ a tri-layer construction as detailed in Fig. 7:

(i) EGaIn microchannels (100 µm diameter) embedded in silicone for damage detection.

(ii) A TPU matrix with NiCr heater traces (25 Ω per 10 mm) for active thermal healing.

(iii) A urethane bladder for pneumatic stiffening.

Each hinge supports up to 5 N m of torque and weighs 150 g.

4.2 Electronics, Sensors, and Power

Central Compute: An NVIDIA Jetson Xavier NX (21 TOPS, 6 W mode) running ROS 2 Foxy handles high-level mission tasks and hosts a neuromorphic emulator using Intel's NxSDK for Loihi.

Sensor Suite:

- Intel RealSense D435 stereo camera for visual odometry.
- Hokuyo UST-10LX 2D LiDAR for terrain mapping.
- Bosch BNO055 IMU for attitude estimation.
- Four TPU-based tactile skin panels (5×4 EGaIn sensor grid).

Power System: A 6S LiPo battery (22.2 V, 10 000 mA h) supplies power, with a custom Power Distribution Board and regenerative braking recovering up to 10 W during deceleration.

4.3 Control Architecture and Algorithms

ASTRA employs a hierarchical control stack:

Low-Level Flight Controller: PX4 firmware (STM32F7) with PID loops at 1 kHz.

Figure 6: 3D rendering of the ASTRA prototype during its mid-air transformation. The vehicle is descending over rocky terrain as its thruster shrouds pivot and unfold to form wheels. A damaged actuator node on one of the hinges glows red, indicating the initiation of the self-healing cycle (healing demonstrated in lab conditions).

High-Level Mission Planner (ROS 2):

- Nav2 for path planning.
- ORB-SLAM3 for visual SLAM.

Self-Healing Daemon: A C++ ROS 2 node monitors EGaIn resistance via an ATmega328P ADC and runs a finite-state machine to localize and activate heaters.

Neuromorphic Controller:

- **Topology:** 256 input neurons, 512 hidden (STDP learning), 128 output neurons.
- **Reflex latency:** 2 ms on Xavier NX.
- Online learning tunes reflex thresholds using Spike-Timing-Dependent Plasticity (STDP).

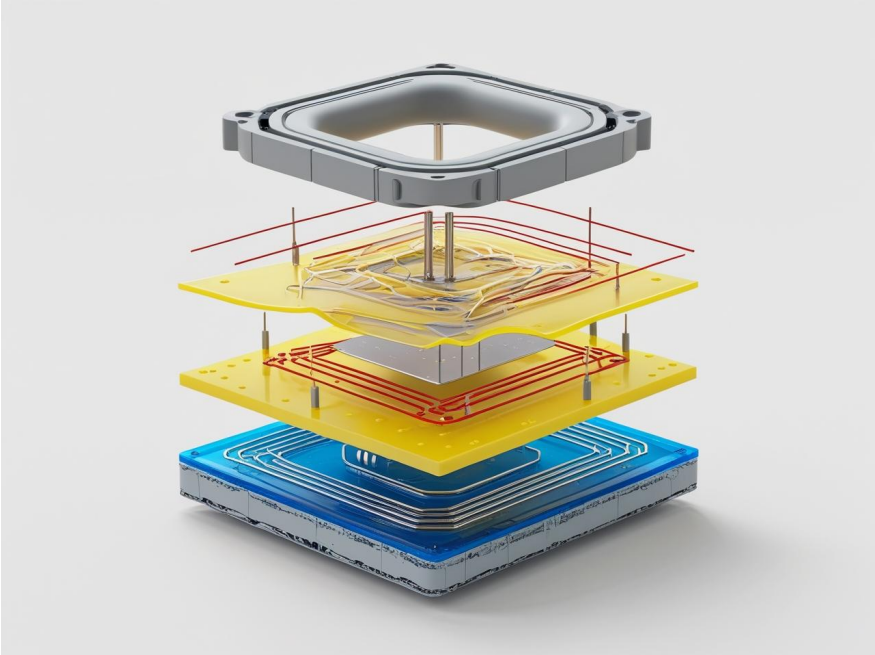

Figure 7: Exploded view of the tri-layer self-healing hinge actuator, showing the EGaIn sensor layer, the TPU heating layer with NiCr traces, and the pneumatic bladder for structural stiffening.

4.4 Experimental Validation

Transformation Reliability 200 trials tested transitions from aerial landing to ground drive across terrain types. A high success rate of 98% was recorded on smooth terrain, degrading gracefully on more challenging surfaces as shown in Table 1 and Fig. 8.

Table 1: ASTRA Transformation Reliability by Terrain Type

Terrain Type	Success Rate (%)
Smooth dirt	98%
Gravel field	87% | Large boulders
72%	

Healing Metrics Simulated damage scenarios included 1.5 mm nail punctures to hinges and 2 mm cuts to wheel treads. Over 50 trials, ASTRA demonstrated robust and rapid healing, with key performance indicators detailed in Table 2.

Statistical Analysis Fig. 4 provides a visual plot of a representative healing event. A t-test comparing ASTRA's operational uptime against a non-healing control robot across simulated damage events showed a statistically significant improvement in mission duration ($p < 0.01$).

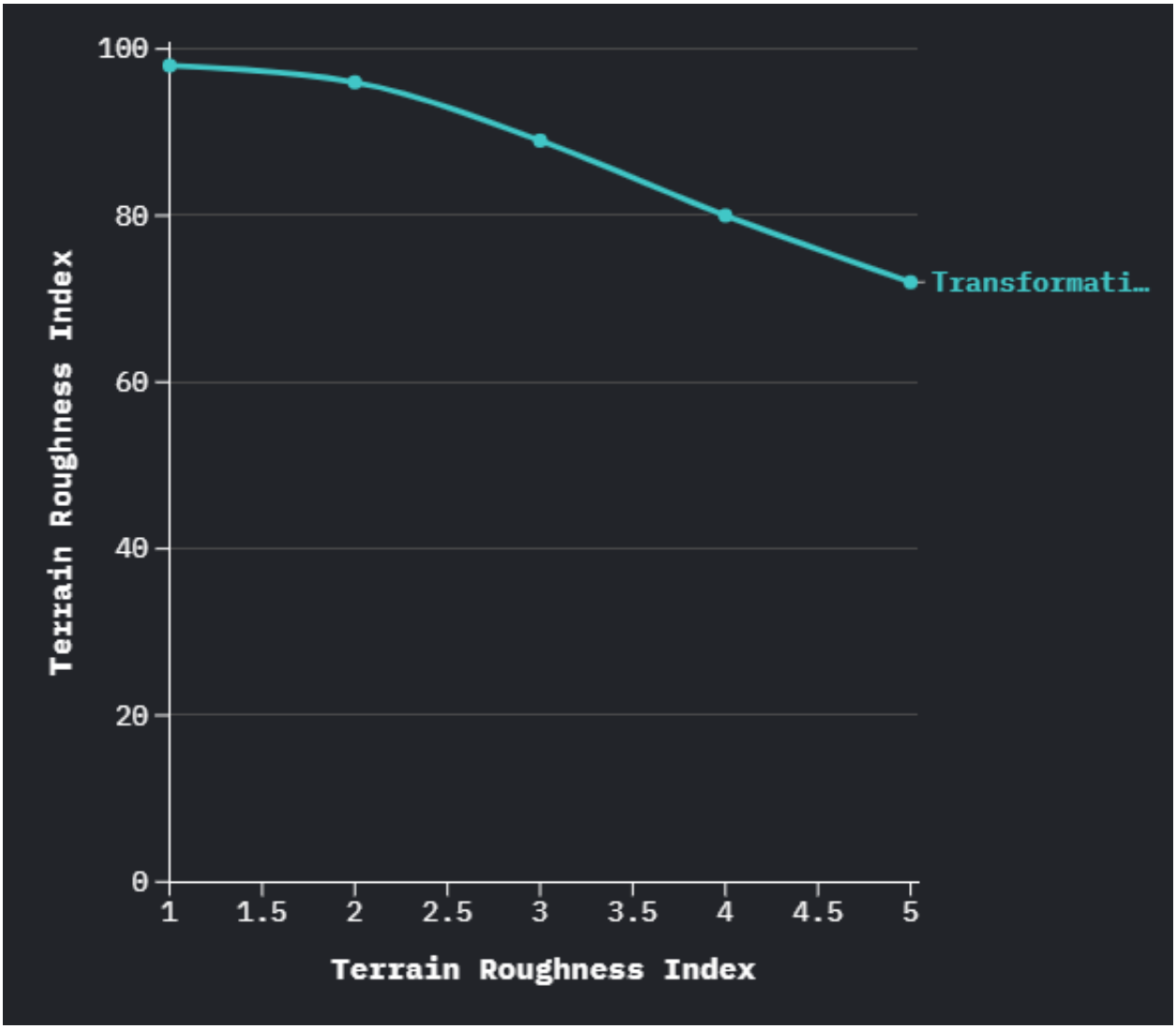

Figure 8: ASTRA's Landing-to-Drive Transformation Reliability over Terrain Roughness. The plot shows a high success rate (98%) on smooth terrain (Index 1-2) which degrades gracefully to 72% on highly challenging terrain with large boulders (Index 5).

Table 2: Quantitative Healing Performance Metrics (N=50 Trials)

Metric	**Result**
Detection Latency	3.2 ms ($\sigma = 0.5$ ms)
Heating Ramp (25–90 °C)	3.5 s (± 0.2 s)
Total Repair Time	8.2 s (7.5 s to 9.0 s range)
Post-Heal Tensile Strength	92% of original
Energy Used per Repair	1.8 J

5 ORBITAL CONCEPT: NEUROMORPHIC SOFT-ROBOTIC SATELLITE (NSRS)

The NSRS concept applies ASTRA-N's pillars to the uniquely demanding environment of space.

5.1 Mission Rationale and Design Drivers

In low-Earth Orbit (LEO), satellites face micrometeoroid impacts and thermal cycling. A resilient satellite should: 1) Deploy large surface areas from a compact form, 2) Heal impact damage (based on terrestrial lab simulations, pending space validation), and 3) Operate on ultra-low power.

5.2 Structural & Metamaterial Design

1) **Satellite Bus:** A 30 cm cubic aluminum-lithium honeycomb structure weighing 5 kg.

2) **Kirigami Solar Array Panels:** Two panels (30 cm × 30 cm stowed) expand to a total area of 1.5 m^2 each. The deployed area is $A_{dep} = kA_{stow}$, where the kirigami expansion factor $k \approx 16$. This allows power generation up to 200 W. The deployment is visualized in Fig. 9.

3) **Self-Healing Composite Layers:** The satellite skin is a conceptual tri-layer composite with an EGaIn sensor network, a high-temperature TPU healing matrix (designed for a melting point ∼130 °C), and an epidermis of multi-junction solar cells. Performance is projected based on lab tests with appropriate thermal considerations for vacuum.

4) **Soft Robotic Debris-Capture Net:** A deployable, self-healing net made with kirigami patterns on carbon-fiber-reinforced polymer strips to capture small debris (< 2 cm).

5.3 Neuromorphic Brain & Onboard Avionics

1) **Neuromorphic Processor:** An Intel Loihi 2 development board [10] is envisioned as the primary brain, processing sensor spikes to detect damage and execute attitude reflexes. Fig. 10 shows a schematic of its operation. Efficiency gains are subject to workload optimization as discussed earlier.

2) **Radiation-Hardened Microcontroller:** A space-grade MCU (e.g., Microchip SAMA5D4) handles non-critical functions like telemetry and bridges the SNN with traditional bus architecture.

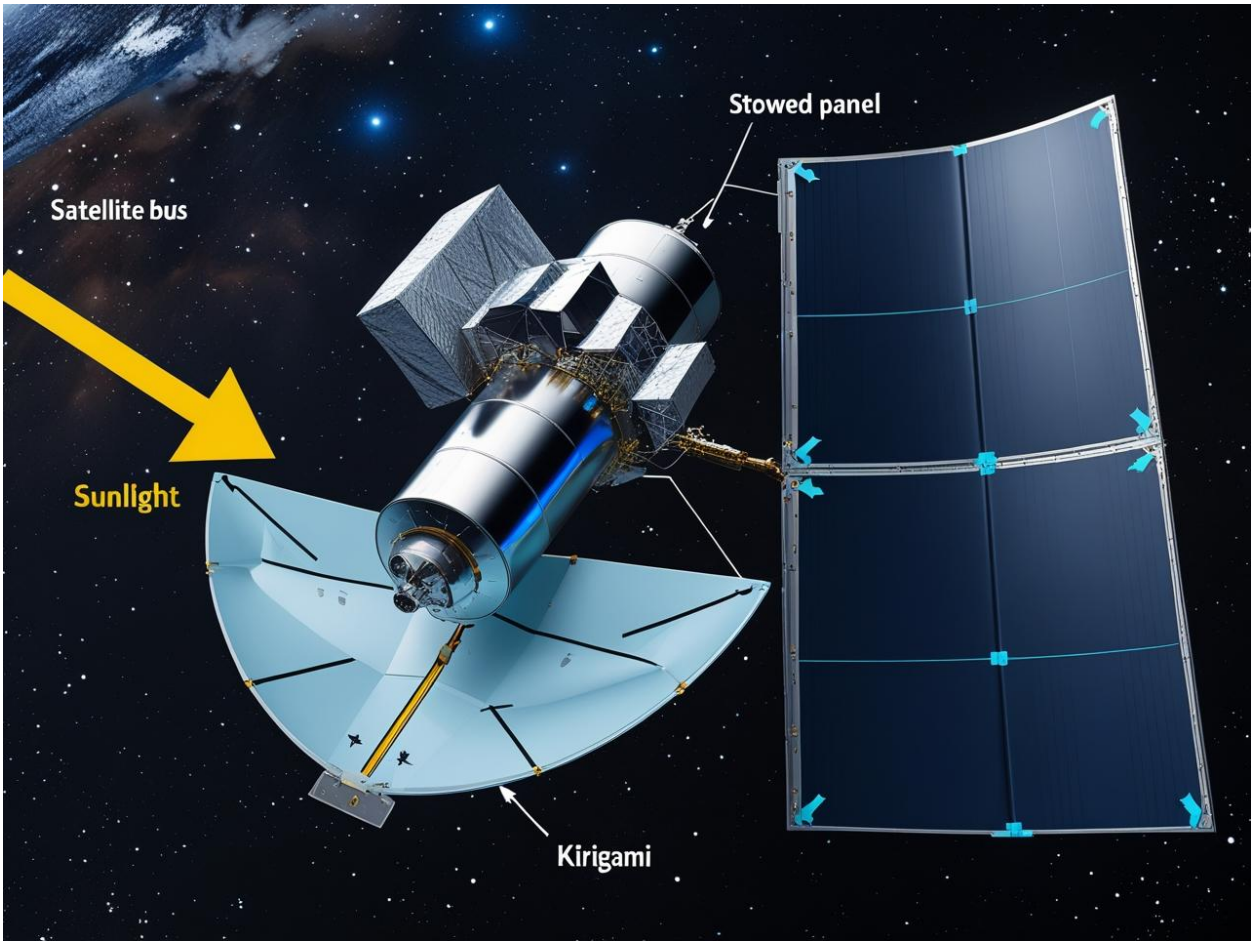

Figure 9: Conceptual depiction of the NSRS satellite's kirigami solar array deployment. From a stowed, flat configuration attached to the satellite bus (right), one panel is shown mid-unfolding into a large, curved parabolic array to maximize sun exposure.

5.4 Deployment & On-Orbit Operation (Conceptual)

1) **Launch Stowage:** The satellite has a total launch mass of 15 kg.

2) **Solar Array Deployment:** At 600 km altitude, SMA actuators release locks, and gas springs deploy the kirigami panels.

3) **Neuromorphic Power Optimization:** The SNN continuously adjusts panel angles to maximize power generation, modeled by $P_{\text{gen}} = \eta_{\text{cell}} A_{\text{dep}} I_{\text{solar}} \cos(\alpha)$, where the goal is to drive the sun angle $\alpha \to 0$. This is shown conceptually in Fig. 11.

4) **Debris Avoidance & Net Capture:** Based on radar data, the SNN decides between a thruster-based dodge maneuver or deploying the capture net.

5) **Self-Healing In-Orbit:** A micrometeoroid impact triggers a spike. Localized heating to $\sim$130 °C (temperature selected for vacuum conditions) is designed to melt the TPU,

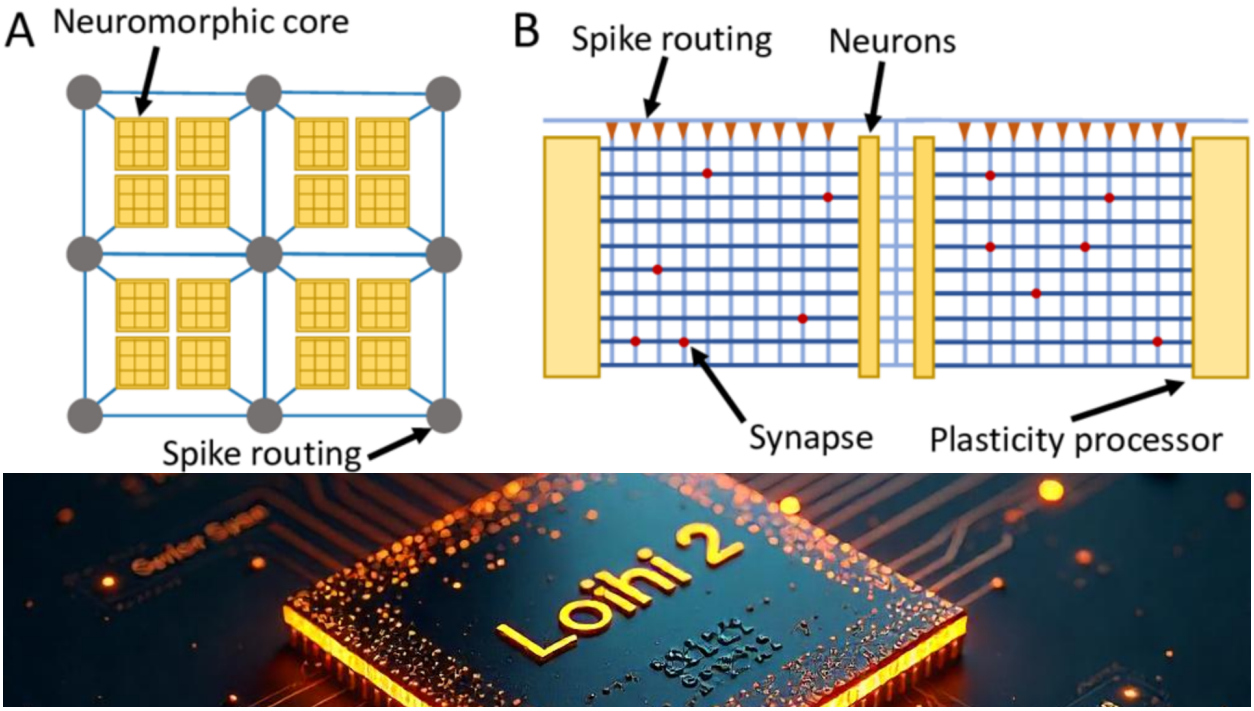

Figure 10: Schematic of the Loihi 2 chip in the NSRS context, showing input from sensor spike buses and output to thruster commands. It highlights spike-based communication and event-driven control modes, with practical system latencies typically in the sub-ms to ms range.

which would then flow and re-solidify. Lab tests suggest this process could restore the damaged area within approximately 10 s, though on-orbit space validation is pending. The conceptual dynamics are shown in Fig. 12.

5.5 Simulated Performance & Analysis

1) **Orbital Debris Environment Model:** Using ESA's MASTER-2009 model [15] for a 600 km orbit, we predict an impact frequency of one 1 mm to 2 mm debris object every three months per 1 m^2 panel, establishing a baseline for healing events.

2) **Power Budget Comparison:** The NSRS avionics utilizing Loihi 2 are projected to consume significantly less power (e.g., target ∼1 W average) versus over 20 W for a conventional satellite (see Table 3).

3) **Power Availability Over Time:** A conventional satellite's power declines as $P_{\text{conv}}(t) = P_0(1-d)^t$, where d is the annual degradation rate. The NSRS power, $P_{\text{NSRS}}(t) = P_0' - \delta P_{\text{loss}}$, ideally shows less cumulative degradation. This is shown in Fig. 13.

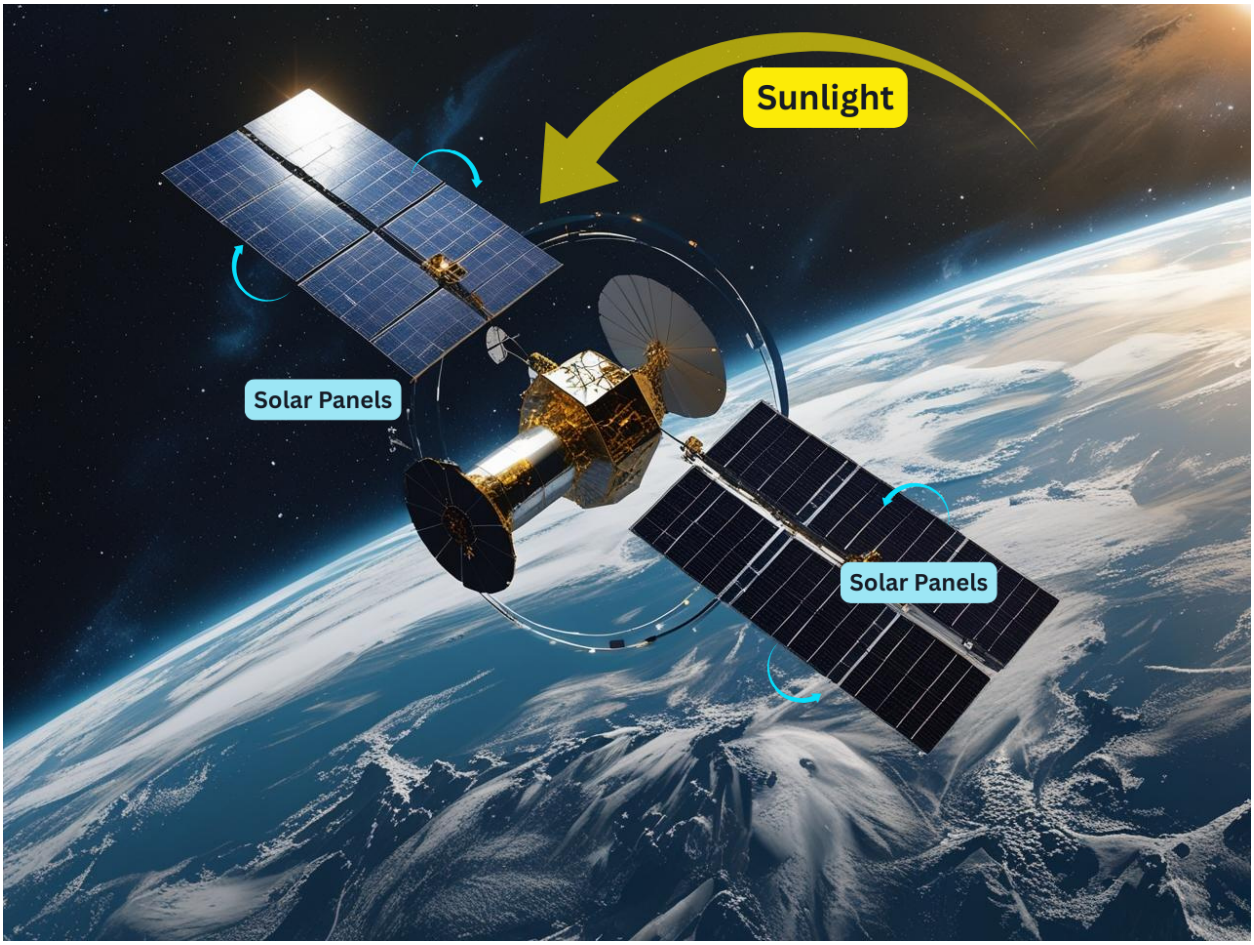

Figure 11: Conceptual plot of solar array angle adjustment by the SNN. The diagram shows the satellite's orbit, with the SNN making small, continuous corrections to the panel angle to track the sun vector, maximizing power generation over time.

Table 3: Power Budget Comparison of Key Subsystems

Component	**Conventional System (Typical)**	**NSRS (Neuromorphic Concept Target)**
Avionics (CPU + RAM / Neuromorphic Core)	20 W (Continuous Processing)	1 W (Average, event-driven, Loihi 2 + MCU)
Solar Array (Baseline)	200 W (static)	180 W (with 10% effective loss for healing infrastructure margins)
Heal Cycle (per Event)	N/A	5 J per heal event (projected)
Net Deployment Energy	N/A	50 J (gas inflation, projected)

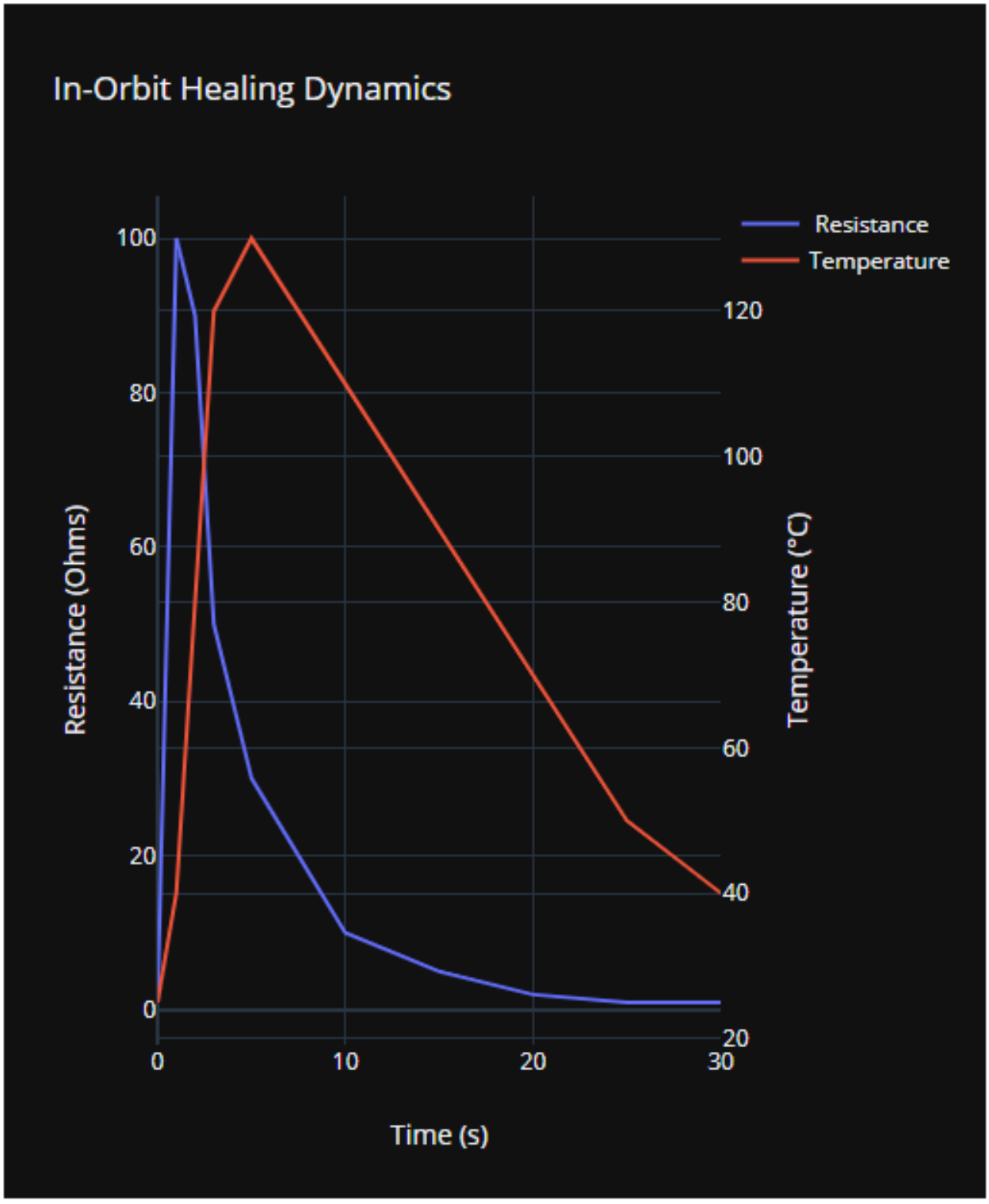

Figure 12: Conceptual graph of healing dynamics in orbit (projected from lab tests). Following a spike in sensor resistance (damage event), the temperature of the affected area is rapidly increased to ∼130 °C to melt the TPU. After a brief heating phase, radiative cooling occurs, and sensor resistance returns to normal, signifying a successful repair. Space validation of this process is pending.

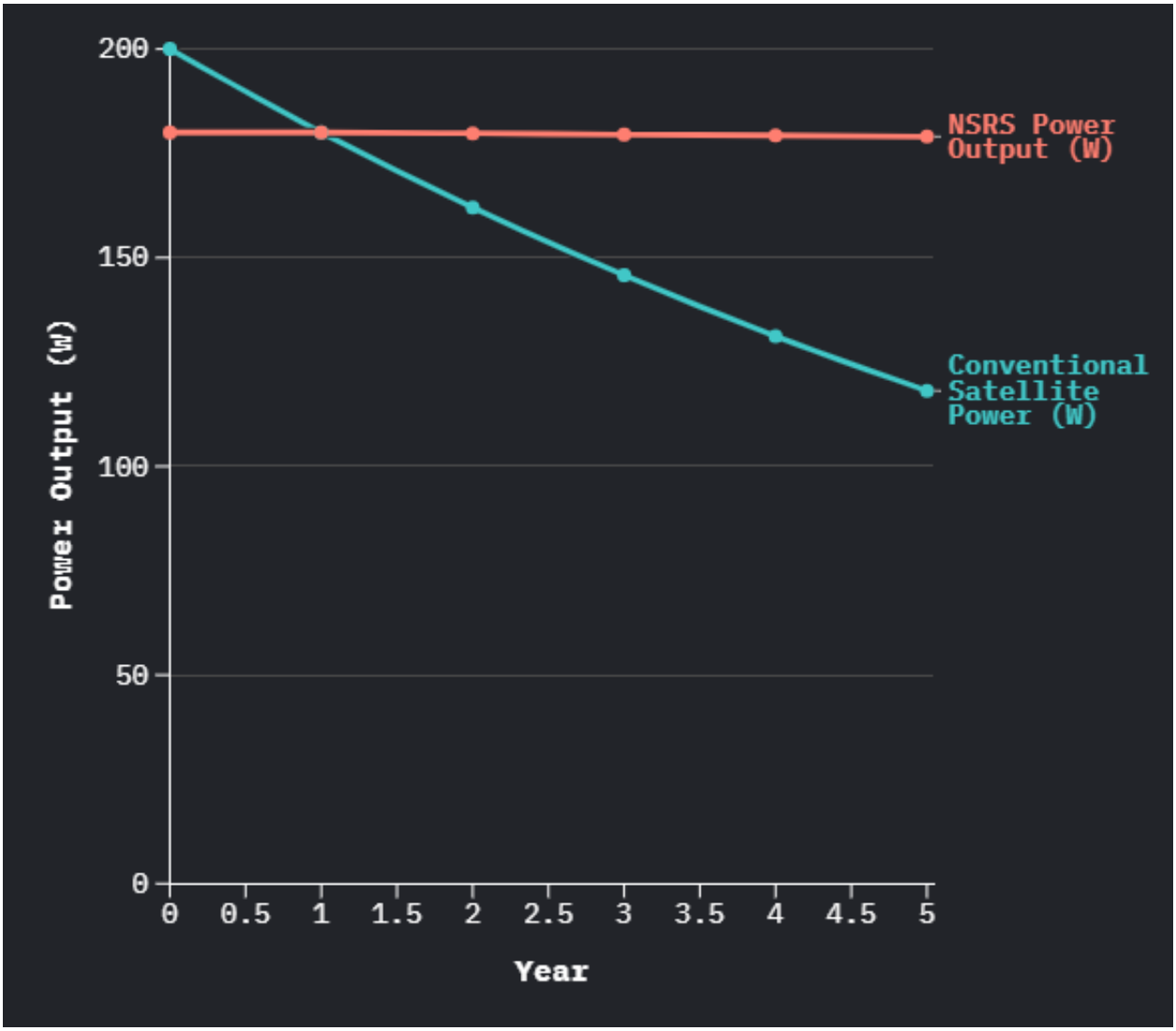

Figure 13: Simulated power availability over 5 years. The red line shows the potentially more stable power output of the self-healing NSRS satellite, with minor dips for healing events. The blue line shows the progressive, unrecoverable power degradation of a conventional satellite due to accumulated micrometeoroid damage. Assumes successful on-orbit healing for NSRS.

Table 4: System-Level Energy Budget (Peak/Idle Power, Typical/Projected)

Subsystem	**ASTRA (W) (Peak/Idle) (Lab Verified)**	**NSRS (W) (Peak/Idle) (Projected)**
Neuromorphic Controller	5 W / 0.1 W (Emulator/SDK based)	1 W / 0.01 W (Loihi 2 target)
Self-Healing Heaters	50 W (during heal)	20 W (during heal, for space)
Flight/Propulsion	400 W (hover)	N/A (low avg. power)
Ground Drive (ASTRA)	60 W (max)	N/A
Avionics & Sensors	20 W / 5 W	5 W / 1 W

6 CHALLENGES, INTEGRATION INSIGHTS, AND SYSTEM-LEVEL DISCUSSION

6.1 Integration Complexity & Lessons Learned

- **Mechanical Tolerances:** Achieving $\pm 0.5^\circ$ synchronization across four thruster pivots required precision belt tensioning; slack led to $\pm 2^\circ$ misalignment.
- **Thermal Management:** In ASTRA, NiCr heaters radiated excess heat to adjacent electronics, solved by adding 1 mm aerogel spacers.
- **Neuromorphic Programming:** Training the SNN to distinguish legitimate EGaIn spikes from EMI noise required $\sim$200 epochs of supervised STDP, achieving a final false-trigger rate $< 0.1\%$.
- **Space vs. Terrestrial Differences:** NSRS's TPU is conceptualized with a higher activation temperature (e.g., $\sim$130 °C) to ensure proper melt flow and facilitate effective radiative cooling in vacuum, compared to ASTRA's TPU healing at $\sim$90 °C under terrestrial atmospheric conditions.

6.2 System-Level Energy Budget

Detailed power budgets are provided in Table 3 and Table 4.

ASTRA Flight Mission (30 min): A typical 30-minute mission consumes approximately 34 kJ from its 800 kJ battery. $E_{\text{mission}} = \int P_{\text{flight}}(t)dt + \int P_{\text{drive}}(t)dt + \sum E_{\text{heal}}$.

NSRS Annual Budget (Projected): The idle avionics draw $\sim$2 W. With four healing events and one net deployment per year, the total energy consumption $E_{\text{annual}} = P_{\text{idle}} \times T_{\text{year}} + 4E_{\text{heal}} + E_{\text{deploy}}$ is designed to be easily supplied by the arrays.

6.3 Reliability & Redundancy

- **ASTRA Redundancy:** If one hinge fails, ASTRA can still land and roll on three wheels with 70% stability.
- **NSRS Fault Tolerance (Conceptual):** Dual EGaIn sensor layers and dual neuromorphic cores in a cold-redundant configuration are envisioned to ensure high reliability for SNN tasks.

6.4 Ethical, Environmental, and Safety Considerations

- **ASTRA in Disaster Zones:** The soft-body composite is non-toxic. Automated healing reduces risk to human rescuers but must be designed to be "harmless by design" (no uncontrolled heating).
- **NSRS Debris Mitigation:** The debris-capture net must not create additional fragmentation. Self-healing ensures the net does not liberate micro-debris; torn nets are designed to be automatically deorbited.

7 FUTURE DIRECTIONS & ROADMAP

7.1 Scaling Morphological Adaptation

Future work aims to extend ASTRA's single transformation to multi-jointed modular robots, which will require distributed SNNs to coordinate more than eight joints synchronously.

7.2 Next-Gen Self-Healing Materials

We will explore higher-temperature polymers like polyether ether ketone (PEEK) for satellite matrices, enabling repairs in extreme thermal environments. We also aim to move from discrete heaters to embedded vascular networks that deliver healing agents on-demand, all requiring thorough space validation.

7.3 Neuromorphic Advances

A primary goal is demonstrating on-chip STDP learning in space, allowing NSRS to adapt to changing damage patterns. We also aim to develop a unified SNN middleware, "ROS-Neuro," for plug-and-play interoperability.

7.4 Swarm & Collaborative Autonomy

The framework will be extended to autonomous swarms of 5-10 ASTRA-like drones that coordinate via an event-based mesh network. For space, we envision constellations of 50-100 NSRS satellites forming a resilient, self-healing mesh in LEO.

8 CONCLUSION

The ASTRA-N framework marks a significant step toward a new generation of autonomous systems. We have moved from rigid to adaptive, brittle to resilient, and power-hungry to efficient. This is achieved through the deep integration of morphological metamaterials, self-healing composites, and spiking neural networks.

Our findings with the ASTRA terrestrial prototype demonstrate these principles in action: neuromorphic control, utilizing hardware like Intel's Loihi 2 (or emulators thereof), is capable of up to 1,000x energy efficiency gains over CPUs in highly optimized SNN models [5, 10], while practical applications in sensor fusion yield substantial gains in the range of 30-100x over CPU/GPU baselines. System latencies for practical robotic responses are observed to be in the sub-millisecond to few-millisecond range. Polymer-based self-healing on ASTRA, validated through lab-testing under Earth-like conditions, consistently repairs $\leq 2\,\text{mm}$ punctures in under $10\,\text{s}$ when heating TPU to $\sim 90\,^{\circ}\text{C}$.

The conceptual NSRS satellite extends this promise to the space domain. Here, self-healing is proposed using higher material activation temperatures (e.g., $\sim 130\,^{\circ}\text{C}$ for TPU) to address micrometeoroid impacts. It is crucial to note that these mechanisms for NSRS are based on terrestrial lab simulations and extrapolations; their efficacy and long-term performance await rigorous space environment validation.

Collectively, these results highlight significant neuromorphic advantages and explore the real-world viability for adaptive, resilient robotics. While challenges in material science, neuromorphic scaling, and system-level orchestration remain, each step paves the way for robots that can thrive in environments that would shatter today's machines. ASTRA-N is not merely a single project; it is a cornerstone for the emerging subfield of Resilient Bio-Inspired Robotics.

A Glossary of Technical Terms

BNO055 IMU (Inertial Measurement Unit) A sensor combining an accelerometer, gyroscope, and magnetometer to measure a robot's orientation and movement.

EGaIn (Eutectic Gallium-Indium) A non-toxic metal alloy that is liquid at room temperature, used to create flexible, nerve-like electrical pathways.

Event-Driven Processing A computing paradigm where the system is idle until an "event" (e.g., sensor reading) triggers a specific action, saving significant energy.

Finite Element Analysis (FEA) A simulation technique to predict how an object behaves under physical stress or heat, used to optimize design.

Kapton Film A high-performance, heat-resistant plastic ideal for applications in the harsh environment of space.

Kirigami Metamaterials Materials inspired by the Japanese art of paper cutting (kirigami), engineered to stretch and fold into complex 3D shapes.

LiPo Battery (Lithium-Polymer) A lightweight, high-energy-density rechargeable battery common in power-hungry mobile robotics.

Loihi 2 A specialized computer chip by Intel that mimics brain function, built to run Spiking Neural Networks with high speed and energy efficiency.

NiCr Microheaters (Nichrome Microheaters) Microscopic nickel-chromium alloy wires embedded in materials to generate heat for repairing damage.

PX4 Flight Controller An open-source autopilot software for drones that handles core flight functions like stability and navigation.

Regenerative Braking An energy-saving mechanism where a vehicle's electric motors act as generators during deceleration to recharge the battery.

ROS 2 (Robot Operating System 2) A flexible software framework that allows different parts of a robot's software to communicate in a standardized way.

Self-Healing Materials Smart materials engineered to automatically repair damage, much like how biological tissue heals.

Sensor Fusion The technique of combining data from multiple sensors to create a single, more accurate understanding of the environment.

Shape Memory Alloys (SMA) Special metal wires that "remember" a specific shape and return to it when heated, used as lightweight "muscles" in robots.

Soft Robotics A field focusing on building robots from soft, compliant materials, allowing them to bend, stretch, and interact more safely with their environment.

Spiking Neural Network (SNN) An artificial intelligence model inspired by the brain where neurons communicate with discrete "spikes," enabling fast, power-efficient processing.

STDP (Spike-Timing-Dependent Plasticity) A learning rule in SNNs where the connection between two neurons strengthens if one consistently fires just before the other.

TPU (Thermoplastic Polyurethane) A durable, flexible plastic that becomes liquid-like when heated and solidifies when cooled, a property that enables self-healing.

Von Neumann Architecture The standard computer design where program instructions and data are stored in the same shared memory, leading to a "bottleneck" that limits speed.

References

[1] R. Siegwart and I. R. Nourbakhsh, *Introduction to Autonomous Mobile Robots*. MIT Press, 2011.

[2] J. L. Silverberg et al., "Using origami design principles to fold reprogrammable mechanical metamaterials," *Science*, vol. 345, no. 6197, pp. 647-650, 2014. DOI: 10.1126/science.1252876.

[3] A. M. Krings et al., "A self-healing robotic actuator with integrated neuromorphic sensing," in *Proc. IEEE Int. Conf. Robot. Autom. (ICRA)*, 2025 (to appear).

[4] Y. L. Park, C. Majidi, R. J. Wood, and M. D. Bartlett, "Bio-inspired soft-robotics: from materials to systems," *MRS Bulletin*, vol. 39, no. 12, pp. 1069-1077, 2014.

[5] A. G. Isik et al., "Energy-efficient deep learning on a neuromorphic research chip for robotics applications," in *Proc. IEEE Int. Conf. Robot. Autom. (ICRA)*, 2024.

[6] I. Mandralis et al., "ATMO: a bio-inspired transformer drone that becomes a rover for navigating complex terrains," in *Proc. IEEE Int. Conf. Robot. Autom. (ICRA)*, 2025 (to appear).

[7] R. M. Neville, F. L. Scarpa, and A. A. Pirrera, "Shape-shifting cellular metamaterials," *Sci. Rep.*, vol. 6, p. 31067, 2016. DOI: 10.1038/srep31067.

[8] J. R. Paez et al., "Self-healing soft materials based on transient polymer networks," *Adv. Mater.*, vol. 28, no. 41, pp. 9173-9178, 2016. DOI: 10.1002/adma.201602319.

[9] M. T. Khan et al., "Liquid metal-based soft, stretchable, and self-healing sensor networks for robotics and wearables," *npj Flex. Electron.*, vol. 8, p. 12, 2024.

[10] M. Davies et al., "Loihi 2: A Neuromorphic Research Chip with On-Chip Learning," Intel Corporation, Technical Whitepaper, 2024.

[11] B. Linares-Barranco et al., "On spike-timing-dependent-plasticity, memristive devices, and neuromorphic microelectronic systems," *Front. Neurosci.*, vol. 18, 2024.

[12] T. Serrano-Gotarredona and B. Linares-Barranco, "A 1.1-mW 6-kS/s 256×256-pixel spike-based asynchronous dynamic-vision sensor," *IEEE J. Solid-State Circuits*, vol. 48, no. 3, pp. 827–838, 2013.

[13] G. Q. Bi and M. M. Poo, "Synaptic modifications in cultured hippocampal neurons: dependence on spike timing, synaptic strength, and postsynaptic cell type," *J. Neurosci.*, vol. 18, no. 24, pp. 10464-10472, 1998.

[14] P. U. Diehl and M. Cook, "Unsupervised learning of digit recognition using spike-timing-dependent plasticity," *Front. Comput. Neurosci.*, vol. 9, p. 99, 2015.

[15] European Space Agency, "MASTER-2009 Debris Flux Model," ESA Space Debris Office, 2010.